

Exciton Quasi-Condensation in One Dimensional Systems

Yochai Werman¹ and Erez Berg¹

¹*Weizmann Institute of Science*

(Dated: November 10, 2018)

A quasi-exciton condensate is a phase characterized by quasi-long range order of an exciton (electron-hole pair) order parameter. Such a phase can arise naturally in a system of two parallel oppositely doped quantum wires, coupled by repulsive Coulomb interactions. We show that the quasi-exciton condensate phase can be stabilized in an extended range of parameters, in both spinless and spinful systems. For spinful electrons, the exciton phase is shown to be distinct from the usual quasi-long range ordered Wigner crystal phase characterized by power-law density wave correlations. The two phases can be clearly distinguished through their inter-wire tunneling current-voltage characteristics. In the quasi-exciton condensate phase the tunneling conductivity diverges at low temperatures and voltages, whereas in the Wigner crystal it is strongly suppressed. Both phases are characterized by a divergent Coulomb drag at low temperature. Finally, metallic carbon nanotubes are considered as a special case of such a one dimensional setup, and it is shown that exciton condensation is favorable due to the additional valley degree of freedom.

PACS numbers:

I. INTRODUCTION

Excitons are bound states between an electron and a positively charged hole. Similar to Cooper pairs, which are bound states of two electrons, excitons are bosons, and may form a condensate. The exciton condensate phase has been studied extensively, both theoretically and experimentally, and in the last few years several groups have reported physical signatures of such a phase in two-dimensional bilayers coupled by Coulomb interactions¹⁻⁴. Two typical experiments are performed in order to probe exciton condensation - counter-flow Coulomb drag³⁻⁵, in which the current flow through only one of the layers is suppressed due to interlayer scattering, and tunneling⁶, whereby the current between the layers is enhanced at low voltages.

Although long-range excitonic order cannot exist in 1D, an exciton quasi-condensate phase (corresponding to a power-law decay of exciton correlations) can occur at zero temperature. Such a phase has definitive signatures in both tunneling and Coulomb drag experiments. In this paper, we consider a system of two parallel quantum wires with an opposite sign of the carriers. We calculate the inter-wire tunneling current-voltage characteristics in different regimes. We show that a divergence of the tunneling conductivity at low temperatures and voltages is intimately linked to exciton quasi-condensation, while a peak in the drag resistance is not. In addition, we consider the special case of a pair of oppositely gated parallel carbon nanotubes, for which we show that exciton quasi-condensation is particularly favorable⁷.

For simplicity, we begin with a spinless model (Section II). The addition of spin in Section III introduces an incompatibility between tunneling and interwire backscattering, resulting in modified $I-V$ curves corresponding to the case of either tunneling or backscattering dominated systems. To conclude, we consider the case of carbon nanotubes (Section IV), which are a natural experimen-

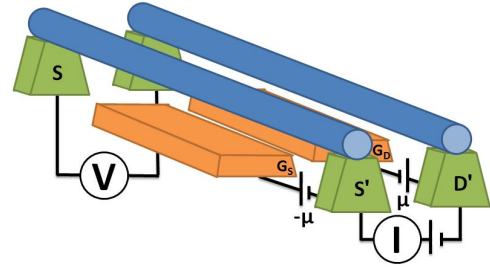


FIG. 1: Proposed setup of the system. The two wires (in this figure - carbon nanotubes) are suspended via the green metallic contacts (color online) above additional gates. The voltage difference between the contacts and the gates controls the doping of the nanotubes, and we choose this voltage to be opposite for the two wires (μ and $-\mu$ in the figure) so that CNT S is electron doped and CNT D hole doped, with the same density of charge carriers. In a tunneling experiment, a voltage difference is placed between contacts S' and D' , forcing a tunneling current between the two nanotubes, which is measured. The resulting voltage difference between the two nanotubes may be read off the voltmeter placed between D and S , which gives $V + 2\mu$, V being the desired quantity.

tal realization of our model, and display an additional electronic degree of freedom - the valley.

II. SPINLESS FERMIONS

A. Model

We commence our analysis with spinless fermions. The theoretical system under consideration is composed of two parallel, infinitely long one dimensional wires, one of

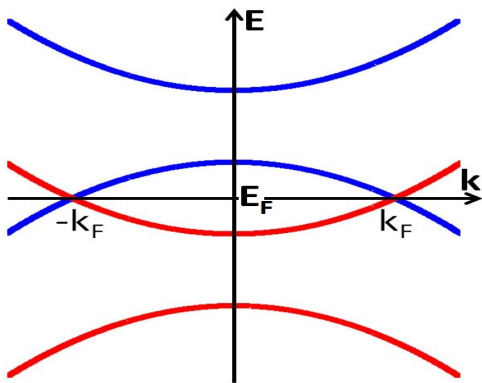


FIG. 2: The dispersion relation for the two wires. The upper, red dispersion (color online) represents the electron-doped wire, while the other is hole doped. The densities of charge carriers are the same for both wires, and therefore k_F is identical. Tunneling between the two wires connects right movers from one wire to left movers from the other. The spectrum is linearized around each Fermi point, and the slopes, equal to the Fermi velocity v_F , are assumed to be of the same magnitude for simplicity.

which is doped with electrons and the other with holes (See Fig.1). The density of carriers in the two wires is identical, so that the Fermi momenta are equal, $k_{F1} = k_{F2}$. The system is described by the Hamiltonian

$$H = H_{\text{kin}} + H_{\text{int}}. \quad (1)$$

Here, $H_{\text{kin}} = -i \sum_{j,\eta} v_F \int dx c_{j\eta}^\dagger (j\eta \partial_x) c_{j\eta}$, where $c_{j\eta}^\dagger$ is the creation operator for a right/left moving ($\eta = \pm 1$) electron in wire $j = \pm 1$; the spectrum has been linearized around k_F . H_{int} is the interaction Hamiltonian, to be specified below. At this stage, we neglect the inter-wire tunneling. A system of two wires coupled by four-fermion interactions (but not by single-electron tunneling) has been studied by various authors (see, e.g., Refs. [8–10]); the new element in the present discussion is the fact that the charges in the two wires are of opposite sign.

It is helpful to revert to the bosonized representation of one dimensional electrons¹¹, where $c_{i\eta}^\dagger \sim e^{i(\eta\phi_i - \theta_i)}$. The bosonic field ϕ_i is related to the electronic charge density fluctuations by $\sum_\eta c_{i\eta}^\dagger c_{i\eta} = \partial_x \phi_i / \pi$. θ_i is similarly related to the electronic current fluctuations. In terms of the bosonic variables, the small momentum (forward scattering) part of the interaction becomes quadratic. The Hamiltonian takes the form $H = H_0 + H_1$, where the quadratic part of the Hamiltonian results in the Tomonaga-Luttinger form

$$H_0 = \sum_{\lambda=\pm} \frac{u_\lambda}{2\pi} \int dx \left[K_\lambda (\partial_x \theta_\lambda)^2 + \frac{1}{K_\lambda} (\partial_x \phi_\lambda)^2 \right], \quad (2)$$

where we have introduced the fields $\phi_\pm = \frac{1}{\sqrt{2}} (\phi_1 \pm \phi_2)$, and the same for θ_\pm . u_\pm are the velocities of the plasmons, and K_\pm are the corresponding Luttinger parameters, given by $K_\pm = \frac{K}{\sqrt{1 \pm UK}}$, where K is the Luttinger parameter of an individual wire (including the effect of the intra-wire interactions). $U = V_{q=0}/2v_F$ is the dimensionless inter-wire forward scattering strength (V_q is the Fourier transform of the inter-wire density-density interaction).

In addition to the forward scattering term, which is quadratic in the bosonic fields, backscattering between the wires is also possible, and gives rise to the term

$$\begin{aligned} H_{BS} &= V_{q=2k_F} \int dx c_{1R}^\dagger c_{1L} c_{-1R}^\dagger c_{-1L} + \text{H.c.} \\ &= -|V_{BS}| \int dx \cos(2\sqrt{2}\phi_+), \end{aligned} \quad (3)$$

where $V_{BS} \propto V_{q=2k_F}$ is the strength of the backscattering interactions. Note the minus sign in Eq. (3), which arises from the commutation relations between the ϕ and θ fields, see Appendix A. If only small momentum scattering is present ($V_{BS} = 0$), the two modes are massless, and the correlations of physical observables decay as power laws for any interaction strength. The operators with the most slowly decaying correlations are the $2k_F$ component of the density, giving rise to the density-density correlation function decaying as $\langle c_{j,+}^\dagger(x) c_{j,-}(x) c_{j,-}^\dagger(0) c_{j,+}(0) \rangle \sim 1/x^{K_+ + K_-}$, and exciton (particle-hole pair) correlations, which satisfy $\langle c_{1,+}^\dagger(x) c_{2,-}(x) c_{2,-}^\dagger(0) c_{1,+}(0) \rangle \sim 1/x^{K_+ + 1/K_-}$.

In the presence of backscattering ($V_{BS} \neq 0$), and if backscattering is relevant (which is the case for $K_+ < 1$), a gap $\Delta_{BS} \propto V_{BS}^{1/(2-2K_+)}$ opens in the spectrum of total charge fluctuations. The partially gapped phase has enhanced Wigner crystalline (density-density) correlations. As we will show, in the spinless case this phase also displays enhanced excitonic correlations.

B. Inter-wire Tunneling

Tunneling current measurements are a sensitive experimental method by which to probe exciton correlations. Tunneling from an external lead into an interacting one dimensional system is normally suppressed^{12–15}; this is a result of the strong correlations between electrons in a Luttinger liquid, which resist the entrance of an external, uncorrelated particle. In our system of two coupled wires, on the other hand, exciton correlations between the two wires tend to enhance the tunnelling current, since particles in one wire are aligned with holes in the other.

In an experiment by Spielman et al.⁶, signatures of exciton condensation have been detected in a two dimensional bilayer subject to a high magnetic field. A sharp

peak in the differential inter-layer tunneling conductivity, $\sigma(V) = \frac{dI_t}{dV}$ (where I_t is the tunneling current density and V the interlayer voltage) at zero bias has been interpreted as a signature of such long-range order¹⁶. Here, we present theoretical predictions regarding the tunneling current-voltage relations in the one dimensional equivalent of the system studied in Ref. [6].

In order to allow for a tunneling current, weak inter-wire hopping is added to the Hamiltonian:

$$H_{\text{tun}} = -\tilde{t}_\perp \sum_{i\eta} \int dx c_{i\eta}^\dagger(x) c_{-i-\eta}(x) = -t_\perp \int dx \cos(\sqrt{2}\phi_+) \sin(\sqrt{2}\theta_-), \quad (4)$$

where \tilde{t}_\perp is the inter-wire tunnelling amplitude, and $t_\perp \propto \tilde{t}_\perp$ (the proportionality constant being $1/(2\pi a)$ in a naive continuum limit, where a is the short distance cutoff). The RG equations for the two non-quadratic terms, the interwire backscattering (3) and tunneling, are:

$$\begin{aligned} \frac{dV_{BS}}{ds} &= [2 - 2K_+] V_{BS} \\ \frac{dt_\perp}{ds} &= \left[2 - \frac{1}{2} \left(K_+ + \frac{1}{K_-} \right) \right] t_\perp \end{aligned} \quad (5)$$

Here s is the momentum scaling parameter, $\Lambda(s) = \Lambda_0 e^{-s}$.

Tunneling is relevant for $K_+ + K_-^{-1} < 4$, which corresponds to a wide range of physical parameters. In this regime, a gap $\Delta_t \propto t_\perp^{1/(2-\frac{1}{2}(K_+ + K_-^{-1}))}$ is opened for fluctuations of the total density and relative charge. In addition, when backscattering is relevant, which is the case for $K_+ < 1$, the fluctuations of the total density are further suppressed, renormalizing the corresponding Luttinger parameter to zero. We assume that the backscattering gap is larger than the tunneling energy scale in the rest of the section.

For energies above Δ_t , or when tunneling is irrelevant, a linear response calculation for the current is applicable. The tunneling current is approximated by¹⁷

$$I_t(V) = 2|t_\perp|^2 \text{Im}\{G_A^{\text{ret}}(q=0, \omega = -eV)\}, \quad (6)$$

Where $G_A^{\text{ret}}(q, t) = -i\Theta(t) \langle [A(q, t), A^\dagger(-q, 0)] \rangle$ and $A(x, t) = c_1^\dagger(x, t)c_{-1}(x, t)$. The linear response calculations result in power laws in the voltage, with the exponents governed by the Luttinger parameters, corresponding to the fact that current dissipates through the excitation of plasmons in the Luttinger liquid. The exponents distinguish between regimes where different sectors are locked; for $\Delta_{BS} \ll eV$, we get $I_t \sim V^{K_+ + 1/K_- - 2}$, while for $\Delta_t \ll eV \ll \Delta_{BS}$ fluctuations in the total density are suppressed, and $I_t \sim V^{1/K_- - 2}$.

If tunneling is relevant, the low voltage behavior ($eV \ll \Delta_t$) is dramatically different. The relative phase field θ_- is locked, signifying that charge may fluctuate

freely between the two wires, without exciting plasmons. In this regime, the perturbative expression for the current, Eq. (6), breaks down.

In order to analyze this case, we use a generalization of the ‘‘tilted washboard’’ model for Josephson junctions¹⁸. Imagine driving a small current density \mathcal{J} between the two wires. The system is described by following effective Hamiltonian:

$$H_{\text{eff}} = H_0 - \int dx [J \sin(\sqrt{2}\theta_-) - \frac{\sqrt{2}}{e} \mathcal{J} \theta_-], \quad (7)$$

where $J = t_\perp \langle \cos(\sqrt{2}\phi_+) \rangle$. (We assume that the field ϕ_+ is pinned to zero by H_{BS} .) According to the Josephson relation, the inter-wire current density operator is given by $eJ \sin(\sqrt{2}\theta_-)$, and the voltage is given by $(\sqrt{2}/e)d\theta_-/dt$. Dissipation occurs by the creation of soliton-antisoliton pairs that dissociate and induce phase slips of 2π in $\sqrt{2}\theta_-$. The voltage is given by

$$V = \frac{2\pi}{e} \Gamma, \quad (8)$$

with Γ the dissociation rate. These propagating soliton-antisoliton pairs correspond to macroscopic quantum tunneling between consecutive minima of the sine-Gordon potential, $\cos(\sqrt{2}\theta_-)$, whose degeneracy is broken by the tunneling current. We have calculated the rate of macroscopic quantum tunneling using the instanton method (see Appendix B for the details of the calculation). The result is $\Gamma \propto e^{-\frac{\alpha}{T}}$, with $\alpha \approx 2.5e\sqrt{\frac{u-K_-}{2\pi}}J$. This leads to the highly singular current-voltage relationship

$$I(V) \propto -\frac{1}{\log(V)}. \quad (9)$$

Here I is the tunneling current and V the interwire voltage.

Lastly, for high enough temperatures such that $T \gtrsim eV$, the low voltage behavior is Ohmic: $I \propto f(T)V$, where $f(T) = T^{-(3-K_+ - 1/K_-)}$; the retarded Green’s function at finite temperatures is given by¹¹

$$G^{\text{ret}}(q=0, \omega) \propto T^{\alpha-2} B\left(-i\frac{\omega}{4\pi T} + \frac{\alpha}{4}, 1 - \frac{\alpha}{2}\right)^2, \quad (10)$$

with $\alpha = K_+ + 1/K_-$, and B the β -function. Expanding to first order in ω , this gives an imaginary part proportional to $T^{\alpha-3}$.

Our results for spinless electrons are summarized in Table I, and a typical $I(V)$ curve is displayed in Fig.3.

The low voltage tunneling current has clear signatures of exciton correlations. When the inter-wire tunneling is relevant, the zero bias conductivity $\lim_{V \rightarrow 0} \frac{dI}{dV}$ diverges at low temperatures. Furthermore, in the regime in which excitonic correlations are strong, the $I - V$ curve may exhibit negative differential conductance for a finite

	$T = 0$			$T \gg \Delta_t, \Delta_{BS}$	
	$\Delta_t \gg V$	$\Delta_{BS} \gg V \gg \Delta_t$	$V \gg \Delta_{BS}$	$V \ll T$	$V \gg T$
Tunneling relevant	$I(V) \propto \frac{-1}{\log(V)}$	$I(V) \propto V^{1/K_- - 2}$	$I(V) \propto V^{K_+ + 1/K_- - 2}$	$I(V) \propto f(T)V$	$I(V) \propto V^{K_+ + 1/K_- - 2}$
Tunn. irrelevant	$I(V) \propto V^{1/K_- - 2} (\Delta_t = 0)$	$I(V) \propto V^{K_+ + 1/K_- - 2}$			

TABLE I: The tunneling current dependence on interwire voltage V for spinless fermions. When $K_+ + 1/K_- < 4$, tunneling is a relevant. For voltages below the tunneling gap Δ_t , the tunneling I-V relationship is a singular function, resulting in a diverging tunneling resistivity. For voltages above the gap, and when tunneling is irrelevant, the I-V curves obey power laws, as expected in one dimensional systems, with the exponents disinguishing between the regime in which the total density is locked by the relevant backscattering process to that in which it is free. The high temperature system displays ohmic behavior at low voltages.

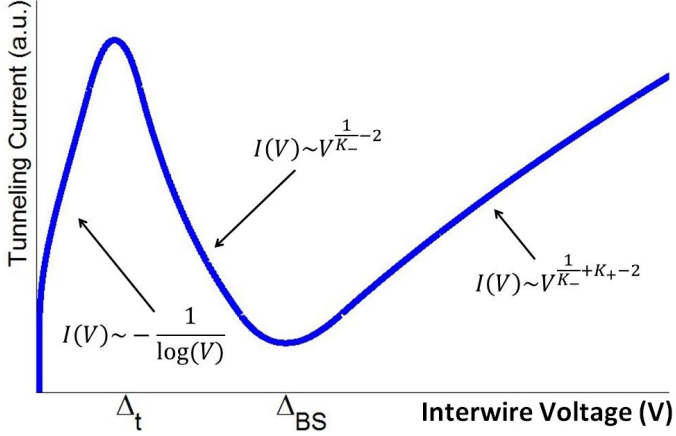


FIG. 3: Current-voltage characteristics for spinless fermions, in the case of relevant interwire tunneling. The tunneling current obeys the singular relationship $I(V) \propto -1/\log(V)$ for voltages lower than the tunneling gap, while at higher voltages it reverts to a power law in the voltage, with the exponent increasing as the difference is amplified. For a large set of values of K_+ , K_- quite accessible experimentally, the exponent may change between a negative and a positive value, as shown in this figure, corresponding to a negative differential conductance for intermediate voltages. This is because in the regime $\Delta_t \ll V \ll \Delta_{BS}$, the total sector is locked by the backscattering gap.

range of voltages, $\Delta_t \ll V \ll \Delta_{BS}$, which may also be interpreted as a mark of exciton quasi-condensation.

III. SPINFUL ELECTRONS

We now consider the case of spinful electrons. The quadratic part of the Hamiltonian is

$$H_0 = \sum_{\mu, \lambda = \pm} \frac{u_{\mu\lambda}}{2\pi} \int dx \left[K_{\mu\lambda} (\partial_x \theta_{\mu\lambda})^2 + \frac{1}{K_{\mu\lambda}} (\partial_x \phi_{\mu\lambda})^2 \right] \quad (11)$$

where, following standard notation, $\phi_{\mu\pm} = \frac{1}{\sqrt{2}}(\phi_{1\mu} \pm \phi_{2\mu})$, $\mu = \rho, \sigma$, where $\phi_{i,\rho/\sigma} = \frac{1}{\sqrt{2}}(\phi_{i\uparrow} \pm \phi_{i\downarrow})$. $\theta_{\rho,\pm}$, $\theta_{\sigma,\pm}$ are defined in a similar fashion. $u_{\sigma\pm}$, $u_{\rho\pm}$ are the velocities of the spin and charge plasmons, and $K_{\sigma\pm}$, $K_{\rho\pm}$ are the corresponding Luttinger parameters. Assuming that there are only density-density inter-wire interactions, spin rotation invariance requires $K_{\sigma\pm} = 1$. The charge Luttinger parameters are $K_{\rho\pm} = \frac{K_\rho}{\sqrt{1 \pm UK_\rho}}$, where K_ρ is the charge Luttinger parameter of an individual wire.

In the spinful model, the $2k_F$ interwire backscattering is adverse to exciton quasi-condensation; it takes the form

$$H_{BS} = \quad (12)$$

$$-|V_{BS}| \int dx \cos(2\phi_{\rho+}) [\cos(2\phi_{\sigma+}) + \cos(2\phi_{\sigma-})],$$

while the tunneling of spinful electrons is described by (see Appendix A)

$$H_{\text{tun}} = t_\perp \int dx [\cos(\phi_{\rho+}) \cos(\phi_{\sigma+}) \cos(\theta_{\sigma-}) \sin(\theta_{\rho-}) - \sin(\phi_{\rho+}) \sin(\phi_{\sigma+}) \sin(\theta_{\sigma-}) \cos(\theta_{\rho-})] \quad (13)$$

It can be seen that the backscattering term tends to lock the field $\phi_{\sigma-}$ (that describes relative spin fluctuations), and therefore it suppressed the transfer of electrons between the wires. Thus the tunnelling and backscattering terms compete with each other in this case. The scaling equations for these two terms are

$$\begin{aligned} \frac{dV_{BS}}{ds} &= [1 - K_{\rho+}] V_{BS}, \\ \frac{dt_\perp}{ds} &= \left[\frac{3}{2} - \frac{1}{4} \left(K_{\rho+} + \frac{1}{K_{\rho-}} \right) \right] t_\perp. \end{aligned} \quad (14)$$

The spinful model leads to two distinct phases, depending on the various Luttinger parameters and initial amplitudes of the non quadratic terms:

1. Tunneling is the dominant interaction: tunneling is more relevant than the $2k_F$ backscattering term for $K_\rho > \frac{1}{3} - \frac{1}{36}U$, and tends to open a gap $\Delta_t \propto t_\perp^{1/(3/2 - 1/4(K_{\rho+} + 1/K_{\rho-}))}$ for fluctuations of the

density in the total sectors and of the phase in the relative sectors.

2. Backscattering is dominant: In this regime, the $2k_F$ backscattering term opens a gap $\Delta_{BS} \propto |V_{BS}|^{1/(1-K_{\rho+})}$ for relative spin fluctuations, which suppresses tunneling up to Δ_{BS} . This phase is characterized by a spin gap and quasi-long ranged charge density waves correlations at wavevector $2k_F$. We denote it as a Wigner crystal.

The zero temperature tunneling current-voltage characteristics of the two phases are shown in Figures 4a and 4b. When the voltage is greater than the gap (either Δ_t or Δ_{BS}), the current follows a powerlaw dependence, $I(V) \propto V^{\frac{1}{2}(K_{\rho+}+K_{\rho-}^{-1}-1)}$. The exponent can have either sign, depending on the strength of the inter- vs. intra-wire interactions. In the backscattering dominated phase, the current goes abruptly to zero when the voltage is below Δ_{BS} . In contrast, in the tunnelling dominated phase, at small voltages the current has a logarithmic dependence on voltage, $I(V) \propto -1/\log(V/\Delta_t)$, as in the spinless case. The tunneling conductivity, $\sigma = \lim_{V \rightarrow 0} \frac{dI}{dV}$, diverges at low voltages.

If the intra-wire interactions are strong, additional backscattering terms arise. In this case, the density correlations in each wire become strongly peaked at a wave vector of $4k_F$, and the amplitude of the $4k_F$ ultimately becomes stronger than the $2k_F$ component¹⁹. The coupling of the $4k_F$ Fourier components of the density in the two wires leads to an additional backscattering term of the form

$$H_{BS,4k_F} = -|V_{BS,4k_F}| \int dx \cos(4\phi_{\rho+}). \quad (15)$$

This term, while less relevant than H_{BS} , has a large amplitude in the strongly interacting limit. In this case, a gap in the $\rho+$ sector can open at an energy larger than Δ_t , Δ_{BS} . In the tunnelling dominated phase, this will result in an $I - V$ curve more similar to the one shown in Fig. 3, with two characteristic energy scales: $\Delta_{BS,4k_F}$ at which the $\rho+$ sector becomes gapped, and Δ_t . We will discuss the effects of the $4k_F$ backscattering term in more detail in a future publication.

Before concluding, let us mention the signatures of the two phases in the drag resistance between the two wires. Although $2k_F$ backscattering suppresses excitonic correlations due to the locking of the relative spin density,

the drag resistance diverges in the backscattering dominated phase at low temperatures^{9,10,20-25}, since the $\phi_{\rho+}$ is locked. In this respect, a divergent drag resistance does not signify enhanced excitonic correlations in our system. The tunnelling dominated phase is insulating at temperatures below Δ_t , so measuring drag resistance is impossible unless a large bias voltage $V > \Delta_t$ is applied to one of the wires.

IV. CARBON NANOTUBES

An obvious experimental realization of the system considered in this work is a double carbon nanotube setup. The two metallic nanotubes can be brought closely together and gated independently. The linearity of the spectrum insures particle-hole symmetry, which favors exciton formation, as such a symmetry results in a nested Fermi surface towards the creation of particle-hole excitations with zero momentum. Finally, carbon nanotubes may be fabricated with an exceptional purity, rendering our neglect of disorder in the previous analysis tenable.

In addition to spin, metallic carbon nanotubes have a valley degree of freedom²⁶. Applying a magnetic field along the axis of the nanotubes lifts the valley degeneracy, as well as the spin degeneracy; one can design systems in which either the valley, the spin, or both are quenched (i.e., only a electrons of a single spin or valley flavour cross the Fermi energy)²⁷. In these cases, the analysis of the previous two sections goes through without modification. Here, we comment briefly on the valley degenerate case (no magnetic field).

Denoting the valley label by $\nu = \pm 1$, we define the boson fields $\phi_{\mu\pm t} = \frac{1}{\sqrt{2}}(\phi_{\mu\pm\nu=1} + \phi_{\mu\pm\nu=-1})$ and $\phi_{\mu\pm r} = \frac{1}{\sqrt{2}}(\phi_{\mu\pm\nu=1} - \phi_{\mu\pm\nu=-1})$, with $\mu = \rho, \sigma$ as before. Intervalley scattering is very much suppressed in carbon nanotubes²⁸, and therefore we assume that $K_{\rho+r} = K_{\sigma+t} = K_{\sigma+r} = K_{\rho-r} = K_{\sigma-t} = K_{\sigma-r} = 1$. The interaction strength is encoded in the Luttinger parameters $K_{\rho\pm t} = \frac{K_{\rho t}}{\sqrt{1 \pm U K_{\rho t}}}$, where $K_{\rho t}$ is the Luttinger parameter for the total charge for a single wire, and U the interwire forward scattering potential.

As in the spinful valleyless case, the interwire backscattering term (16) tends to lock both total (+) and relative (-) modes, and thus competes with the tunneling term (17). The backscattering term is written as

$$H_{BS} = -|V_{BS}| \times [\cos(\sqrt{2}\phi_{+\rho t}) \cos(\sqrt{2}\phi_{+\rho r}) (\cos(\sqrt{2}\phi_{+\sigma t}) \cos(\sqrt{2}\phi_{+\sigma r}) + \cos(\sqrt{2}\phi_{-\sigma t}) \cos(\sqrt{2}\phi_{-\sigma r})) + \cos(\sqrt{2}\phi_{+\rho t}) \cos(\sqrt{2}\phi_{-\rho r}) (\cos(\sqrt{2}\phi_{+\sigma t}) \cos(\sqrt{2}\phi_{-\sigma r}) + \cos(\sqrt{2}\phi_{-\sigma t}) \cos(\sqrt{2}\phi_{+\sigma r}))], \quad (16)$$

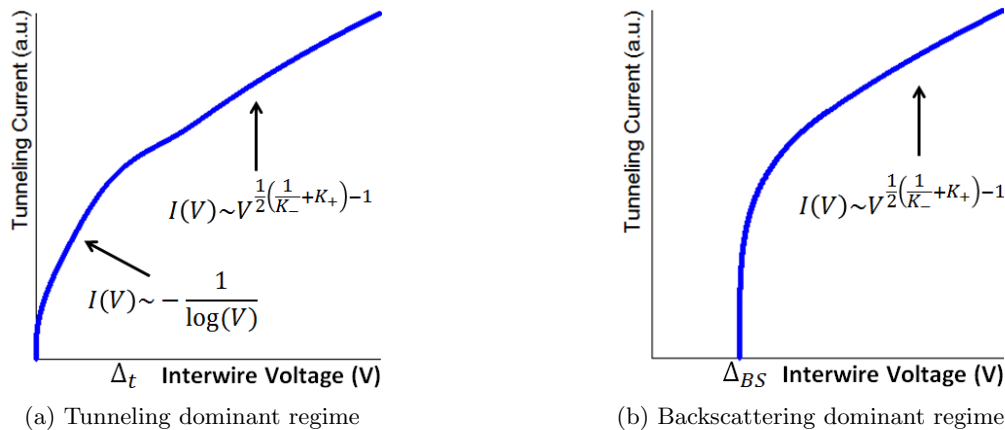


FIG. 4: $I - V$ curve for spinful electrons in the regimes where tunneling or backscattering is dominant. In the tunneling dominant regime, the low voltage current obeys the singular relationship $I(V) \propto \frac{-1}{\log(V)}$, as the current dissipates through the macroscopic tunneling mechanism described in Section II. At high voltages, the current is a powerlaw in the voltage, $I(V) \propto V^{\frac{1}{2}(K_{\rho+} + K_{\rho-}^{-1}) - 1}$. The presence of noninteracting spin sectors ($K_{\sigma} = 1$), and interwire forward scattering U , may decrease the exponent to negative values, resulting in a negative differential conductance. In the regime where backscattering is dominant, the interaction opens a gap Δ_{BS} for relative spin fluctuations which suppresses tunneling up to that scale. At $V \gg \Delta_{BS}$, the current obeys the powerlaw $I(V) \propto V^{\frac{1}{2}(K_{\rho+} + K_{\rho-}^{-1}) - 1}$.

while the inter-wire tunnelling term has the form

$$H_{tun} = t_{\perp} \sin\left(\frac{\phi_{+\rho t}}{\sqrt{2}}\right) \cos\left(\frac{\phi_{+\rho r}}{\sqrt{2}}\right) \cos\left(\frac{\phi_{+\sigma t}}{\sqrt{2}}\right) \cos\left(\frac{\phi_{+\sigma r}}{\sqrt{2}}\right) \cos\left(\frac{\theta_{-\rho t}}{\sqrt{2}}\right) \cos\left(\frac{\theta_{-\rho r}}{\sqrt{2}}\right) \cos\left(\frac{\theta_{-\sigma t}}{\sqrt{2}}\right) \cos\left(\frac{\theta_{-\sigma r}}{\sqrt{2}}\right) + \dots, \quad (17)$$

where the ellipsis stands for terms in which an odd number of cosines is exchanged with sines. The lowest order β -functions of the two terms are given by

$$\begin{aligned} \frac{dV_{BS}}{ds} &= \frac{1}{2} [1 - K_{+\rho t}] V_{BS}, \\ \frac{dt_{\perp}}{ds} &= \left[\frac{5}{4} - \frac{1}{8} \left(K_{\rho+} + \frac{1}{K_{\rho-}} \right) \right] t_{\perp}. \end{aligned} \quad (18)$$

The addition of internal degrees of freedom, such as valley, enhances the possibility for exciton condensation, as was already seen in Section III; the phase where the tunneling conductivity is the most divergent corresponds to intrawire Luttinger parameters obeying $K_{\rho} > 0.15 - 0.01U$ for small U . This regime is accessible in experiments; the experimental estimates for the Luttinger parameter of single walled nanotubes^{13,29} are in the range $K_{\rho} \sim 0.2 - 0.3$, resulting in a more divergent tunneling operator, and thus the tunneling dominated phase may be reached. In this phase, the low voltage tunneling current will obey the familiar $I(V) \propto \frac{-1}{\log(V)}$ law, while for voltages much higher than any emergent gap in the system, the current will again be a power law in the voltage, with the exponent modified by the additional noninteracting sectors, resulting in $I(V) \propto V^{\frac{1}{4}(K_{\rho+t} + K_{\rho-t}^{-1}) - \frac{1}{2}}$.

V. CONCLUSION

In conclusion, we consider a system of oppositely doped wires in the limit of strong forward scattering and weak interwire backscattering and tunneling. For strong enough interwire interactions, the system is susceptible to excitonic quasi-long range order. We further discuss the tunneling current-voltage characteristics, and show that there are three different regimes, depending on the relative relevance and magnitude of the tunneling process and the two types of interwire backscattering. When the tunneling process is dominant, corresponding to a phase with strong excitonic correlations, the zero bias conductivity diverges, making tunneling a sensitive probe of interwire phase coherence. On the other hand, we argue that the drag resistance will diverge both in the excitonic regime and in the Wigner crystal, where the phases of the two wires are independent. Lastly, we examine carbon nanotubes, and note that they are exceptionally suited for the detection of excitons.

Acknowledgments

We thank S. Ilani and B. Rosenow for useful discussions. This work was supported by the Israel Science Foundation, the Minerva fund and a Marie Curie Career Integration Grant (CIG).

Appendix A: Sign Issues

In bosonization theory, electrons of the same species obey fermion statistics due to the commutation relations of the bosons ϕ and θ , while the anticommutation of different species must be put in by hand¹¹. One way to achieve this is to impose the following relationship between θ s of different electrons³⁰:

$$[\theta_i(x), \theta_j(x')] = i\pi\epsilon_{ij}, \quad (\text{A1})$$

where ϵ_{ij} is the antisymmetric tensor.

1. Interwire backscattering

One consequence of the anticommutation of fermions is the sign of the backscattering term. Consider the operator

$$\begin{aligned} c_{1R}^\dagger(x)c_{1L}(x) &\propto & (\text{A2}) \\ \exp(i(\phi_1(x) - \theta_1(x))) \exp(-i(-\phi_1(x) - \theta_1(x))) \\ &= \exp(2i\phi_1(x)) e^{\frac{i}{2}[\phi_1(x) - \theta_1(x), -\phi_1(x) - \theta_1(x)]}, \end{aligned}$$

where the second term on the last line is a consequence of the Baker-Hausdorff formula. The commutator can be evaluated easily using the convention

$$[\phi(x), \theta(x')] = i\pi\Theta(x - x') \quad (\text{A3})$$

along with the point-splitting technique¹¹; it results in

$$c_{1R}^\dagger(x)c_{1L}(x) \propto -i \exp(2i\phi_1(x)). \quad (\text{A4})$$

Therefore,

$$\begin{aligned} c_{1R}^\dagger(x)c_{1L}(x)c_{2R}^\dagger(x)c_{2L}(x) &\propto & (\text{A5}) \\ i \exp(2i\phi_1(x)) \times i \exp(2i\phi_2(x)) &= \\ -\exp\left(2\sqrt{2}i\phi_+(x)\right), \end{aligned}$$

incurring a minus sign that is absent for wires doped equally with the same kind of charge carrier, where backscattering is of the form $c_{1R}^\dagger c_{1L} c_{2L}^\dagger c_{2R}$.

2. Tunneling

The form of the tunneling term is also affected by the fermionic phase:

$$\begin{aligned} c_{1R}^\dagger c_{2L} &\propto e^{i(\phi_1 + \phi_2 - \theta_1 + \theta_2)} e^{\frac{i}{2}[\theta_1, \theta_2]} \\ &= i e^{i(\phi_1 + \phi_2 - \theta_1 + \theta_2)}, \end{aligned} \quad (\text{A6})$$

with equivalent phases for the other three components of the tunneling interaction, which result in the form given by equation (4). The addition of spin generates terms of the form

$$c_{1R\uparrow}^\dagger c_{2L\downarrow} = e^{i(\phi_{\rho+} - \theta_{\rho-} + \phi_{\sigma+} - \theta_{\sigma-})} e^{\frac{i}{4}([\theta_{1\rho}, \theta_{2\rho}] + [\theta_{1\sigma}, \theta_{2\sigma}])}, \quad (\text{A7})$$

resulting again in a factor i , and leading to equation (13).

Appendix B: Instanton calculation

The real time action governing the evolution of the relative phase is given by

$$\begin{aligned} S &= \frac{u_- K_-}{2\pi} \int dx dt \left(\frac{1}{u_-^2} (\partial_t \theta_-)^2 - (\partial_x \theta_-)^2 \right) \\ &+ \int dx dt \left[J \sin(\sqrt{2}\theta_-) + \frac{\sqrt{2}}{e} \mathcal{J} \theta_- \right], \end{aligned} \quad (\text{B1})$$

where, as in section II, $J = t_\perp \langle \cos(\sqrt{2}\phi_+) \rangle$ and \mathcal{J} is the current density driven between the wires, which breaks the symmetry between the minima of the sine-Gordon potential.

The decay rate of the metastable state $\sqrt{2}\theta_0 = \frac{\pi}{2}$ can be calculated from the Green's function $G(T) = \langle \theta_0 | e^{iHT} | \theta_0 \rangle$, which after analytic continuation becomes

$$G(\tau) = \langle \theta_0 | e^{H\tau} | \theta_0 \rangle = \int \mathcal{D}[\theta(\tau')] e^{-S_E[\theta(\tau')]}, \quad (\text{B2})$$

where the Euclidean action S_E is given by

$$\begin{aligned} S &= \frac{u_- K_-}{2\pi} \int dx d\tau \left(\frac{1}{u_-^2} (\partial_\tau \theta_-)^2 + (\partial_x \theta_-)^2 \right) \\ &- \int dx d\tau \left[J \sin(\sqrt{2}\theta_-) + \frac{\sqrt{2}}{e} \mathcal{J} \theta_- \right]. \end{aligned} \quad (\text{B3})$$

We evaluate this path integral by a saddle point approximation, corresponding to field configurations $\{\theta_-(x, \tau)\}$ which satisfy the Euler-Lagrange equations

$$\partial_\tau^2 \theta + \frac{1}{r} \partial_\tau \theta = -\frac{\sqrt{2}\pi}{uK} \left[J \cos(\sqrt{2}\theta) + \frac{\mathcal{J}}{e} \theta \right], \quad (\text{B4})$$

where we have defined $r = \sqrt{x^2 + u^2 \tau^2}$.

For $\mathcal{J} \ll eJ$, meaning that the potential minimum

asymmetry imposed by the current \mathcal{J} is small, it is possible to use the thin wall approximation³¹; in this case, it is assumed that the configurations which minimize the action are described by a domain wall of thickness Δr which is positioned at $r_0 \gg \Delta r$, which separates regions of homogenous configurations of θ - $\theta(r < r_0) = \frac{\pi}{2}, \theta(r > r_0) = \frac{5\pi}{2}$. In this case, the second term in the left hand side of Eq. B4 is much smaller than the first, and the Euler-Lagrange equations are

$$\partial_r^2 \theta \approx -\frac{2\sqrt{2}\pi}{uK} \left[J \cos(\sqrt{2}\theta) + \frac{\mathcal{J}}{e} \theta \right]. \quad (\text{B5})$$

The configurations satisfying this equation are known as instantons, and they describe kinks in the otherwise constant configuration of the θ field. Their action consists of two parts:

1. The action cost of the kink, which scales as $2\pi r_0$, as the kink occurs only along the domain wall. It may be calculated for $\mathcal{J} = 0$ with the assistance of the Euler-Lagrange equation, and results in

$$S_0 \approx 2.5 \sqrt{\frac{uK}{2\pi}} J \quad (\text{B6})$$

2. The action cost of the field being in a metastable minimum, which has an energy larger by $\Delta\epsilon = 2\pi \frac{\mathcal{J}}{e}$. This contribution scales as πr_0^2 , which is the size of the domain in which the field is in the higher energy state.

Therefore, the total action which corresponds to a propagating domain wall in the presence of a nonvanishing current is

$$S = 2\pi r_0 S_0 - \pi^2 r_0^2 \frac{\mathcal{J}}{e}. \quad (\text{B7})$$

The minimum of this action occurs for $r_0 = S_0 / (\pi \frac{\mathcal{J}}{e})$,

and corresponds to the total action

$$S = \frac{S_0^2 e}{\mathcal{J}}. \quad (\text{B8})$$

However, this action is not the only contribution to the path integral that can be obtained from the saddle point approximation. Since the kink of the instanton is localized in time, it is feasible to assume that any number of instantons, separated such that they can be considered as non interacting in the sense that the total action is simply the addition of n single instanton actions S_{inst} ; is also a saddle point configuration. The path integral that is obtained for the Green's function (A2) is therefore

$$\begin{aligned} G(\tau) &\approx \sum_n C^n \int_0^\tau d\tau_1 \dots \int_0^{\tau_{n-1}} d\tau_n e^{-nS} \\ &= \sum_n \frac{1}{n!} (C\tau e^{-S})^n \\ &= e^{C\tau e^{-S}} \end{aligned} \quad (\text{B9})$$

where the n -fold integration occurs due to space-time translation invariance; the value of r at which the kink occurs can vary between 0 and r for $r \rightarrow \infty$. C is a dimensional constant which arises from the Gaussian fluctuations around the minima of action, and from normalization factors.

Applying the analytic continuation, and relying on the fact that K must be pure imaginary³¹,

$$G(t) \propto e^{-t|C|e^{-S}}, \quad (\text{B10})$$

and it follows that the tunneling rate from the metastable minimum is

$$\Gamma = |C| e^{-S} \propto e^{-\frac{S^2 e}{\mathcal{J}}}. \quad (\text{B11})$$

¹ J. P. Eisenstein and A. H. MacDonald, *Nature* **432**, 691 (2004).

² J. A. Seamons, D. R. Tibbetts, J. L. Reno, and M. P. Lilly, *Applied Physics Letters* **90**, 052103 (2007), URL <http://scitation.aip.org/content/aip/journal/apl/90/5/10.1063/1.2437664>.

³ D. Nandi, A. D. K. Finck, J. P. Eisenstein, L. N. Pfeiffer, and K. W. West, *Nature* **488**, 481 (2012).

⁴ K. D. Gupta, A. F. Croxall, J. Waldie, et al., *Advances in Condensed Matter Physics* **2011** (2011).

⁵ D. Laroche, G. Gervais, M. P. Lilly, and J. L. Reno, *Science* **343**, 631 (2014), <http://www.sciencemag.org/content/343/6171/631.full.pdf>, URL <http://www.sciencemag.org/content/343/6171/631.abstract>.

⁶ I. B. Spielman, J. P. Eisenstein, L. N. Pfeiffer, and K. W. West, *Phys. Rev. Lett.* **84**, 5808 (2000), URL <http://>

link.aps.org/doi/10.1103/PhysRevLett.84.5808.

⁷ This is a one-dimensional analogue of the setup proposed by: H. Min, R. Bistritzer, S. Jung-Jung, and A. H. MacDonald, *Phys. Rev. B* **78**, 121401 (2008).

⁸ D. G. Shelton and A. M. Tsvelik, *Phys. Rev. B* **53**, 14036 (1996), URL <http://link.aps.org/doi/10.1103/PhysRevB.53.14036>.

⁹ R. Klesse and A. Stern, *Phys. Rev. B* **62**, 16912 (2000), URL <http://link.aps.org/doi/10.1103/PhysRevB.62.16912>.

¹⁰ M. Pustilnik, E. G. Mishchenko, L. I. Glazman, and A. V. Andreev, *Physical Review Letters* **91**, 126805 (2003), [cond-mat/0208267](http://arxiv.org/abs/cond-mat/0208267).

¹¹ T. Giamarchi, *Quantum Physics in One Dimension* (Clarendon Press, 2003).

¹² D. N. Aristov, A. P. Dmitriev, I. V. Gornyi, V. Y. Kachorovskii, D. G. Polyakov, and P. Wölfle, *Phys. Rev. Lett.*

- 105, 266404 (2010), URL <http://link.aps.org/doi/10.1103/PhysRevLett.105.266404>.
- ¹³ M. Bockrath, D. H. Cobden, J. Lu, A. G. Rinzler, R. E. Smalley, L. Balents, and P. L. McEuen, *Nature* **397**, 598 (1999).
- ¹⁴ O. M. Auslaender, A. Yacoby, R. de Picciotto, K. W. Baldwin, L. N. Pfeiffer, and K. W. West, *Science* **295**, 825 (2002), <http://www.sciencemag.org/content/295/5556/825.full.pdf>, URL <http://www.sciencemag.org/content/295/5556/825.abstract>.
- ¹⁵ Y. Jompol, C. J. B. Ford, J. P. Griffiths, I. Farrer, G. A. C. Jones, D. Anderson, D. A. Ritchie, T. W. Silk, and A. J. Schofield, *Science* **325**, 597 (2009), <http://www.sciencemag.org/content/325/5940/597.full.pdf>, URL <http://www.sciencemag.org/content/325/5940/597.abstract>.
- ¹⁶ T. Hyart and B. Rosenow, *Phys. Rev. B* **83**, 155315 (2011), URL <http://link.aps.org/doi/10.1103/PhysRevB.83.155315>.
- ¹⁷ G. D. Mahan, *Many-Particle Physics* (Springer Science, 2000).
- ¹⁸ M. Tinkham, *Introduction to Superconductivity*, Dover books on physics and chemistry (Dover Publications, 2004), ISBN 9780486435039, URL <http://books.google.co.il/books?id=k6A09nRYbioC>.
- ¹⁹ S. R. White, I. Affleck, and D. J. Scalapino, *Phys. Rev. B* **65**, 165122 (2002), URL <http://link.aps.org/doi/10.1103/PhysRevB.65.165122>.
- ²⁰ R. G. Pereira and E. Sela, *Phys. Rev. B* **82**, 115324 (2010), URL <http://link.aps.org/doi/10.1103/PhysRevB.82.115324>.
- ²¹ S. Teber, *Phys. Rev. B* **76**, 045309 (2007), URL <http://link.aps.org/doi/10.1103/PhysRevB.76.045309>.
- ²² K. Flensberg, *Phys. Rev. Lett.* **81**, 184 (1998), URL <http://link.aps.org/doi/10.1103/PhysRevLett.81.184>.
- ²³ Y. V. Nazarov and D. V. Averin, *Phys. Rev. Lett.* **81**, 653 (1998), URL <http://link.aps.org/doi/10.1103/PhysRevLett.81.653>.
- ²⁴ V. V. Ponomarenko and D. V. Averin, *Phys. Rev. Lett.* **85**, 4928 (2000), URL <http://link.aps.org/doi/10.1103/PhysRevLett.85.4928>.
- ²⁵ G. A. Fiete, K. Le Hur, and L. Balents, *Phys. Rev. B* **73**, 165104 (2006), URL <http://link.aps.org/doi/10.1103/PhysRevB.73.165104>.
- ²⁶ S. Dresselhaus, G. Dresselhaus, and P. Avouris, *Carbon Nanotubes: Synthesis, Structure, Properties, and Applications*, Physics and astronomy online library (Springer, 2001), ISBN 9783540410867, URL <http://books.google.co.il/books?id=dkvDhZJnafgC>.
- ²⁷ F. Kuemmeth, S. Ilani, D. C. Ralph, and P. L. McEuen, *Nature* **452**, 448 (2008), ISSN 7186, URL <http://dx.doi.org/10.1038/nature06822>.
- ²⁸ C. Kane, L. Balents, and M. P. A. Fisher, *Phys. Rev. Lett.* **79**, 5086 (1997), URL <http://link.aps.org/doi/10.1103/PhysRevLett.79.5086>.
- ²⁹ Z. Yao, H. W. C. Postma, L. Balents, and C. Dekker, *Nature* **402**, 273 (1999).
- ³⁰ J. von Delft and H. Schoeller, *Annalen der Physik* **7**, 225 (1998), ISSN 1521-3889, URL [http://dx.doi.org/10.1002/\(SICI\)1521-3889\(199811\)7:4<225::AID-ANDP225>3.0.CO;2-L](http://dx.doi.org/10.1002/(SICI)1521-3889(199811)7:4<225::AID-ANDP225>3.0.CO;2-L).
- ³¹ A. Altland and B. Simons, *Condensed Matter Field Theory* (Cambridge University Press, 2010).